Hydration activation of Alite-Belite-Ye'elimite cements by doping with boron

Journal:	*ACS Sustainable Chemistry & Engineering*
Manuscript ID	sc-2019-05975t.R2
Manuscript Type:	Article
Date Submitted by the Author:	n/a
Complete List of Authors:	Zea-Garcia, Jesus D.; Universidad de Malaga Facultad de Ciencias, Inorganic Chemistry Sanfelix, Susana; Ostfold University College, Faculty of Engineering Vallcorba, Oriol; ALBA Synchrotron Light Source, Aranda, Miguel; Universidad de Malaga, QUIMICA INORGANICA Santacruz, Isabel; Universidad de Malaga, Química Inorgánica, Cristalografía y Mineralogía De la Torre, Angeles; Universidad de Malaga,

Hydration activation of Alite-Belite-Ye'elimite cements by doping with boron

*Jesus D. Zea-Garcia[a], Susana G. Sanfelix[b], Oriol Vallcorba[c], Miguel A.G. Aranda[a], Isabel Santacruz[a], Angeles G. De la Torre[a,]**

[a] Departamento de Química Inorgánica, Cristalografía y Mineralogía, Universidad de Málaga, Facultad de ciencias, Campus Teatinos, Málaga, 29010, Spain.

[b] Faculty of Engineering, Østfold University College, N-1757 Halden, Norway

[c]ALBA Synchrotron, Carrer de la Llum 2-26. 08290 Cerdanyola del Vallès, Barcelona, Spain

* email: mgd@uma.es

KEYWORDS: Ecocements; calcium sulfoaluminate; boron effect; retardant; synchrotron radiation; X-ray diffraction; solid state MAS-NMR; calorimetric study; C-S-H gel; compressive strength.

ABSTRACT

The hydration behavior of two alite-belite-ye'elimite (ABY) cements has been studied. The production of these materials releases into atmosphere ~17% less CO_2 than Portland cement. ABY

cement contains alite, β-C_2S and ye'elimite as main phases while dABY (activated by adding borax) contains these three phases but also α'_H-C_2S. The role of boron in these systems is two-fold: i) acting as a retarder at early hydration ages, since the precipitation of AH_3-gel has been delayed from over 4 hours in ABY to over 24 h in dABY; and ii) as an activator at late hydration ages by stabilizing highly reactive β- and α'_H-belites. The degree of hydration of β-C_2S in ABY is 42% at 28 days, meanwhile that of β-C_2S and α'_H-C_2S in dABY at the same age is 80 and 88%, respectively. Moreover, the main hydration products in both systems are ettringite and C-S-H gel. The local structure of these hydrated products have been studied by ^{27}Al and ^{29}Si MAS-NMR and found to be similar in both cements. However, the amount of C-S-H gel is 63% of all silicon bearing phases in ABY after 28 days while is 76% (determined by ^{29}Si MAS-NMR) in dABY which justifies the higher mechanical strengths of dABY mortars.

Introduction.

The challenge of reducing greenhouse emissions is one of the most important issues that scientists are facing. Portland Cement (PC) production releases up to ~0.98 tons of CO_2 per ton of cement type-I manufactured, taking into account the limestone calcination (0.54 tons), the burning of the fossil fuels (0.34 tons) and the electricity for grinding (0.09 tons). Thus, the cement industry is responsible of ~7% of the total CO_2 emissions due to human activities[1–3]. There are several approaches to reduce these emissions[4], such as lowering the amount of clinker in the final cement by blending with Supplementary Cementitious Materials (SCMs)[5] or modifying the raw materials and consequently, the chemical composition of the final product[2]. The main component of PC is Ca_3SiO_5 (alite or C_3S) which is a high calcium demanding phase. Calcite is the main calcium source in cement production and CO_2 comes from the decarbonation of calcite in the kilns. Hereafter, the cement nomenclature will be adopted: C=CaO, S=SiO_2, A=Al_2O_3, F=Fe_2O_3, $\bar{S}$=SO_3

and H=H_2O. Alite hydration products are the main responsible of the high mechanical strengths developed by PC at early ages. Calcium sulfoaluminate ($C_4A_3\bar{S}$ or ye'elimite) containing cements are included in the second approach, as this phase is a less calcite demanding phase.[4,6] In the recent years, an economical and environmental alternative known as Belite-Ye´elimite-Ferrite (BYF) cements have been proposed[7–10]. These BYF cements usually contain belite, C_2S (>50 wt%) and ye'elimite (~30 wt%), as their main phases. A reduction of 0.15 tons of CO_2 due to decarbonation of raw materials in the kiln is achieved in the production of BYF cements. Additionally, the lower clinkering temperature and the more friable material obtained cause a reduction of 0.06 extra tons of carbon dioxide due to the burn of the fuel and the consumption of electricity during milling. The development of these materials is still under research[11,12] due to three main issues; i) the early hydration of ye'elimite phase with anhydrite or gypsum and the rheological behavior should be controlled to obtain the desired mechanical performances[13], ii) the durability performances are still unknown and likely related to those of calcium sulfoaluminate cements[14] and iii) the development of mechanical strengths with a strength gain vs time similar to that of PC by activation/enhancing the reactivity of the main phase, i.e. belite.[10,15,16] There has been several approaches to achieve this latter goal, stabilizing α-polymorphs of C_2S by the inclusion of foreign elements in the structure [10,17,18] (for instance B_2O_3 and Na_2O) or by the increase of sulfate content in the raw mix[16,19]. The main aim of these strategies is to stabilize α'_H-C_2S which is more hydraulically active at early ages[20]. A step forward in the activation of these materials is the production of cements with coexistence of alite, belite and ye'elimite (ABY)[21–24]. The main idea of these types of materials is to profit from the early mechanical strength development due to the hydration of alite. However, the clinkering of ABY binder is challenging since the optimum temperature for the alite formation

is above the decomposition temperature of ye'elimite.[25] This drawback has been overcome by adding fluorite to the raw mix[26,27] jointly with other minor elements.[28–33]

Moreover, there is still lack of information on the properties of fresh pastes of ye'elimite based materials. The addition of additives to control the setting time and/or the rapid increase of viscosity is of great importance in order to achieve high mechanical strengths[34,35]. The addition of retarders such as boric acid or citric acid provokes a diminution of the 1 day mechanical strengths but an increase in the later ages when compared with the mortars without any additive[13,36].

In this work, the early hydration of two ABY cements has been characterized. These ABY cements have been prepared following the two described activation approaches, i.e the presence of alite and ye'elimite and the addition of boron to stabilize the α-polymorphs of C_2S. The hydration behavior and the nature of main hydrated phases have been studied and correlated to mechanical properties.

Experimental Procedure.

Cement preparation.

ABY and dABY clinkers were prepared by clinkering raw mixtures at 1300ºC for 15 minutes as detailed elswhere[37]. The elemental compositions of the clinkers are given in Table 1.

Table 1. Nominal elemental compositions, expressed in weigh percentage of oxides excluding water and CO_2, of all raw mixtures used to prepare ABY clinkers.

Clinker	CaO	SiO_2	SO_3	Al_2O_3	Fe_2O_3	MgO	K_2O	Na_2O	ZnO	CaF_2	B_2O_3
ABY	58.9	19.8	5.4	10.7	1.6	0.8	0.8	--	1.0	1.0	--
dABY	58.4	19.6	5.3	10.6	1.6	0.8	0.8	**0.3**	1.0	1.0	**0.6**

Both clinkers were grinded with 14 wt% of anhydrite to prepare the cements (being this the stoichiometric amount of calcium sulfate needed for full reaction with ye'elimite/aluminates to yield ettringite). The anhydrite used was a commercial bassanite from BELITH S.P.R.L. (Belgium) heated at 700°C for 60 min. Blaine parameters of the final cements were 374 and 294 m^2/kg for ABY and dABY, respectively. Figure S1, given as supplementary material, shows the particle size distribution (PSD) of both cements, being $D_{v,50}$ and $D_{v,90}$ 9.1 and 67.6 μm and 9.8 and 75.3 μm, respectively. PSD measurements were carried out in a laser diffraction analyzer (MastersizerS, Malvern) provided with a dry sample cell at Financiera y Minera cement factory (Heidelberg group, Malaga, Spain).

Paste preparation.

Two different pastes preparations were carried out to perform the *in-situ* and *ex-situ* hydration studies with the selected water to cement (w/c) mass ratio of 0.5.

For the *in-situ* study, both anhydrous cements were mixed with 12 wt% of SiO_2 (99.5%, AlfaAesar) as internal standard with a McCrone micronizing mill[38] to indirectly determine the overall amount of amorphous and non-crystalline (ACn) component of the pastes[38]. Both pastes were prepared by mixing the sample (cement + internal standard) with the corresponding amount of water by hand in a small plastic beaker for 2 min using a spatula and then immediately loaded into glass capillaries of 0.7 mm of diameter with a syringe. The capillaries were sealed with grease to avoid any water loss.

For the *ex-situ* study, cement pastes were prepared with deionized water following a modified UNE-EN 196-3 methodology, where a mechanical stirrer was used with fixed speed of 800 rpm[37]. The pastes were poured into hermetically closed polytetrafluoroethylene (PTFE) cylinders, and were rotated (16 rpm) during the first 24 h at 20±1ºC[37]. Afterward, hardened pastes were placed

into a bath of water at 20±1ºC to be used at the selected curing ages (4 and 15 hours, and 1, 7, 28, 90 days). The hydration of the samples was stopped before their characterization: samples were manually grinded, and washed twice with isopropanol, once with diethyl ether and finally dried at 40ºC for 24 hours in a stove.

Synchrotron X-ray powder diffraction (SXRPD).

An *in-situ* hydration study for both ABY and dABY cements was carried out by SXRPD. Patterns were collected in the beamline MSPD-BL04 located at ALBA synchrotron (Barcelona, Spain). Patterns were recorded in Debye-Scherrer (transmission) mode[39] with a wavelength of 0.61931(3) Å (20 keV). The diffractometer is equipped with a MYTHEN detector system especially suited for time-resolved experiments and good signal-to noise ratio. The data acquisition time was 6 min per pattern. The glass capillaries were rotated at 20 rpm during data collection to improve diffracting particle statistics. Two patterns per hour (of 6 minutes each) were collected at different hydration times, during the first 14 hours, over the angular range from 2 to 40° (2θ). Normalized SXRPD patterns were analysed by using the Rietveld methodology in order to obtain Rietveld Quantitative Phase Analysis (RQPA). Figures S2.a and S3.a show the raw SXRPD patterns of ABY and dABY pastes.

Laboratory X-ray Powder Diffraction (LXRPD)

The LXRPD measurements were carried out on both anhydrous cements and stopped hydration pastes. A X'Pert MPD PRO PANalytical diffractometer with Copper radiation with a Johansson Ge(111) primary monochromator that yields to monochromatic $CuK\alpha_1$ (λ = 1.5406 Å) was used. The diffractometer was located at Servicios Centrales de Apoyo a la Investigación (SCAI) at University of Malaga (Spain). Data were collected from 5º to 70° (2θ) with a measuring time of

2.5 hours. Samples were spun during data collection at 16 rpm. Figures S2.b and S3.b show the raw LXRPD patterns of ABY and dABY stopped pastes.

Data analysis

Firstly, LXRPD or SXRPD patterns were qualitatively studied, identifying the cementitious crystalline phases with X'Pert High Score Plus program from PANalytical with reference patterns from PDF database. Subsequently, the patterns were analyzed by Rietveld method using GSAS software package[40] by using a pseudo-Voigt peak shape function with the asymmetry correction included[41,42], to obtain RQPA. The refined overall parameters were: background coefficients, zero-shift error, phase scale factors, unit cell parameters, peak shape parameters and preferred orientation coefficient if needed. The structure descriptions of crystalline phases used are given elsewhere[37]. Figures S4 and S5 show Rietveld plots of ABY and dABY pastes after 1 and ~14 hours of hydration (*in-situ* study), respectively, as representative examples.

The determination of ACn was performed by two methods: i) by the internal standard methodology[38] in the *in-situ* study, and ii) the external standard method (G-factor approach)[38,43] in the *ex-situ* study of the pastes at 1, 7, 28, 90 days of hydration.

Rheological behavior of cement pastes.

A viscometer (Model VT550, Thermo Haake, Karlsruhe, Germany) with a serrated coaxial cylinder sensor, SV2P, provided with a lid to reduce evaporation, was used.

A rheological study was carried out to understand the behavior of these two cements pastes at very early hydration time, prepared at the w/c ratio of 0.5, without the addition of any superplasticizer. The study of the effect of superplasticizer on the hydration of these cements is published elsewere[35].

Two measurements were performed with this device: i) flow curves (controlled rate measurements) where ramp times of 6 s were recorded in the shear rate range between 2 and 350 s^{-1}, for a total of 12 ramps (up-curve). A further decrease from 350 to 2 s^{-1} shear rate was performed by following the same ramp times (down-curve). Prior to any measurement, pastes were pre-sheared at 350 s^{-1} for 30 s and held at 0 s^{-1} for 5 s. The data were acquired after ~5 min from adding water to the cement powder. ii) Viscosity vs. time measurements, at a fixed shear rate of 5 s^{-1}.

Magic Angle Spinning Nuclear Magnetic Resonance (MAS-NMR) study

^{29}Si MAS-NMR spectra for ABY and dABY samples were recorded at room temperature on a Bruker AVIII HD 600 NMR spectrometer (field strength of 14.1 T) at 119.8 MHz with a 2.5 mm triple-resonance DVT probe using zircona rotors at 15 kHz spinning rate. The experiments were performed with ^{1}H decoupling by applying single-pulse excitation with a $\pi/2$ pulse of 5 us, 30 s relaxation delay and 10800 scans. The chemical shift was referenced to an external solution of tetramethylsilane (TMS).

^{27}Al MAS-NMR spectra were recorded in the same spectrometer at 156.4 MHz and the rotors operated at 20 kHz. The experiments were performed with and without ^{1}H decoupling (cw sequence) by applying a single pulse ($\pi/12$), an excitation pulse of 1 μs and 5.0 s relaxation delay and 200 scans. The chemical shift was referenced to an external solution of 1 M of $Al(NO_3)_3$.

The ^{29}Si- MAS-NMR spectra were analysed using DMFIT software[44] with a deconvolution scheme of Gaussian fitting into several peaks for the anhydrous and hydrated phases.

Isothermal calorimetry

This study was performed in an eight channels Thermal Activity Monitor (TAM) instrument using glass ampoules. In order to collect data from the very beginning of the hydration an

automatic admix device was used to mix the samples inside the calorimeter by shaking the sample during the first 2 minutes. The heat flow was collected up to 7 days at 20°C.

Results and discussion.

Early hydration behaviour: first hour.

Figure 1 displays the flow curve of both pastes. At the first minutes of hydration, ABY paste shows higher viscosity and thixotropic cycle than the dABY one (viz. viscosity values were 1.92 and 0.93 Pa·s at 100 s^{-1}, taken from the up-curves, and thixotropic cycles of 5201 and 2202 Pa/s, for ABY and dABY, respectively). The higher viscosity of ABY paste at this very early hydration time may be attributed to i) the smaller primary particle size[37], ii) the lower (agglomerate) size of this cement (Figure S1) and consequently slightly higher Blaine parameter, which is related with higher particle interactions, and iii) slightly higher initial amount of total ye'elimite, Figure 2 and Tables S1 and S2, deposited as supplementary information.

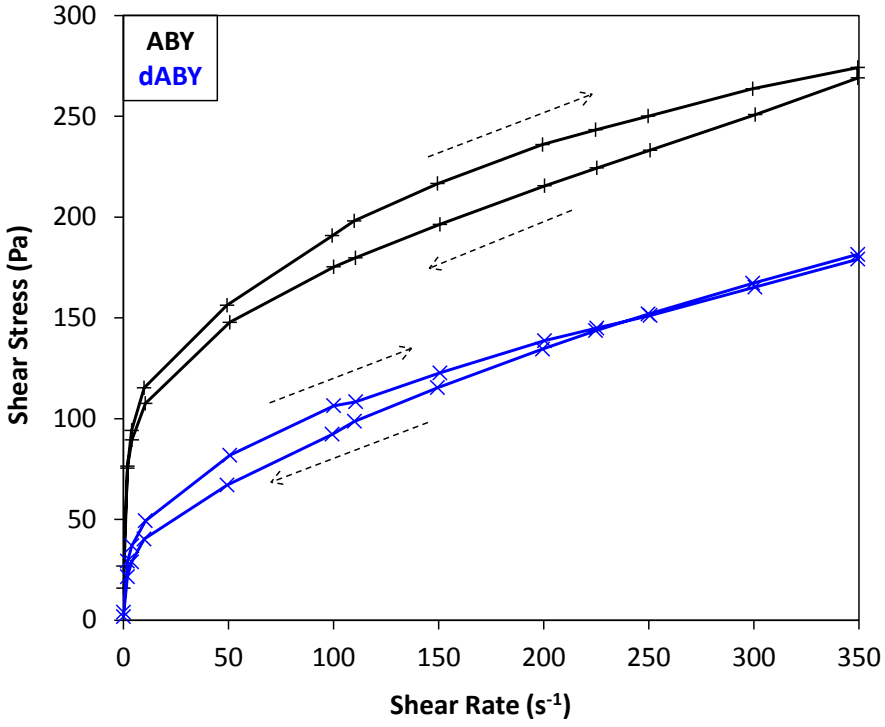

Figure 1. Flow curves for ABY and dABY pastes at w/c of 0.5. ABY in black; dABY in blue.

However, after 10 minutes of hydration, dABY paste suffers a harsh increase in viscosity, as can be observed in Figure 3 (left axis), even higher than that for ABY paste. That figure shows the evolution of viscosity with time (left axis), data from Zea et al.[35], and the cumulative heat in the first 24 hours of hydration. This viscosity increase is in agreement with the higher cumulative heat released by dABY up to 3 hours of hydration. This behavior can be explained through the higher dissolution/reactivity degree of some phases, especially mayenite. Moreover, the presence of $C_{12}A_7$ accelerates the hydration of ye'elimite[45]. The SXRPD patterns, given in Figure S2 and S3 as Supporting Information, were analyzed and Figure 2 shows the phase assembly of main phases of both pastes obtained from the *in-situ* synchrotron radiation data analyses (full RQPA results given in Tables S1 and S2 as Supporting Information). Figure 2 shows that $C_4A_3\overline{S}$ has almost totally dissolved after 1 day in both cements to form ettringite and amorphous aluminum hydroxide, which is included in the ACn content. In systems with silicates and calcium sulfoaluminate, the hydration of alite and belite may yield a silicate rich hydration environment where AFt decomposed[21,46]. This effect is observed after 24 hours of hydration and an increase in ACn is observed in both cements, Figure 2.

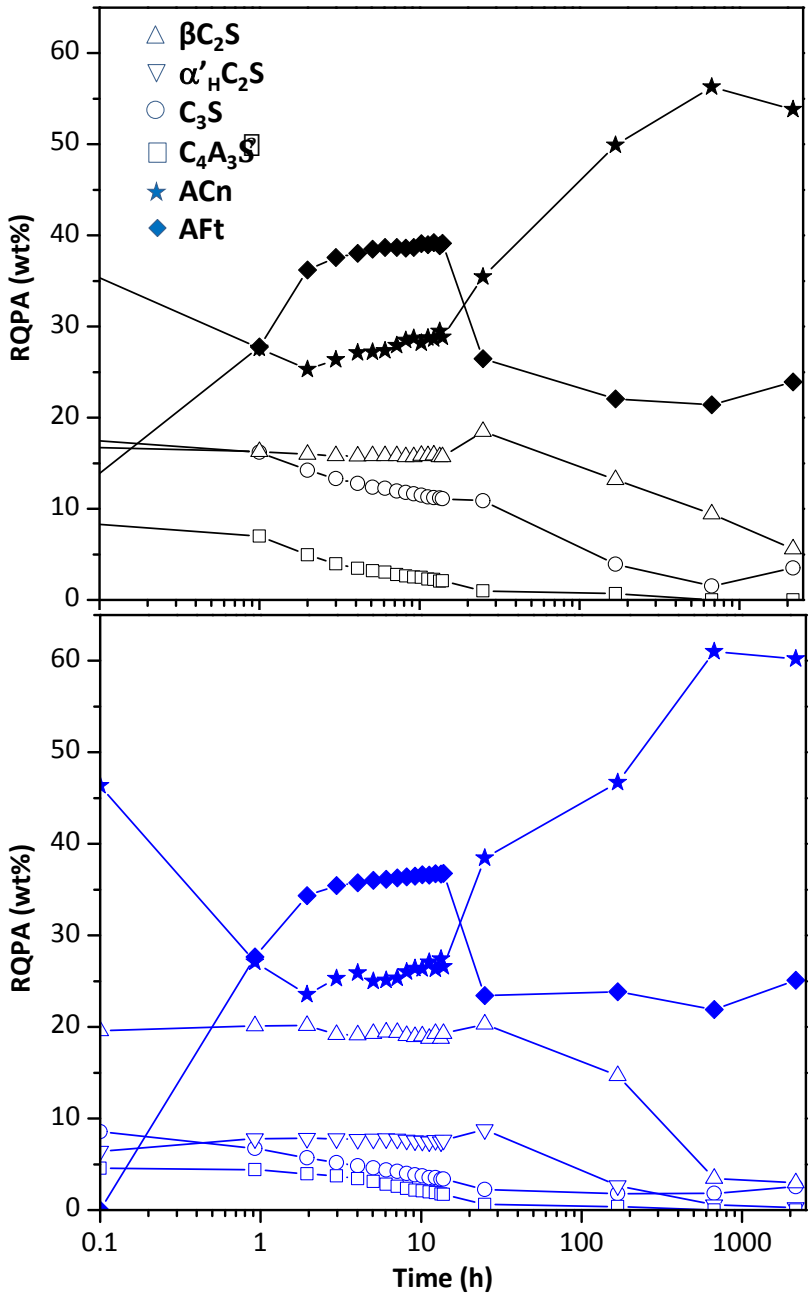

Figure 2. Phase assemblage as a function of time for ABY (up) and dABY (down), where only main phases are plotted.

Figure 3 also shows the degree of reaction of C_3S in the first 14 hours of hydration determined from the data given in Tables S1 and S2. On the one hand, the presence of a small amount of

mayenite in dABY cement is the responsible of the accelerated formation of ettringite and the increase of viscosity in the first 30 minutes of hydration[45], Table S2 and Figure 3. On the other hand, the degree of hydration of alite in dABY cement, which contains less amount of total ye'elimite, is always higher than in ABY, Figure 3. This is mainly due to fact that the kinetic of alite hydration is affected by the presence of ye'elimite[47], where the higher the amount of ye'elimite the slower early age reactivity of alite.

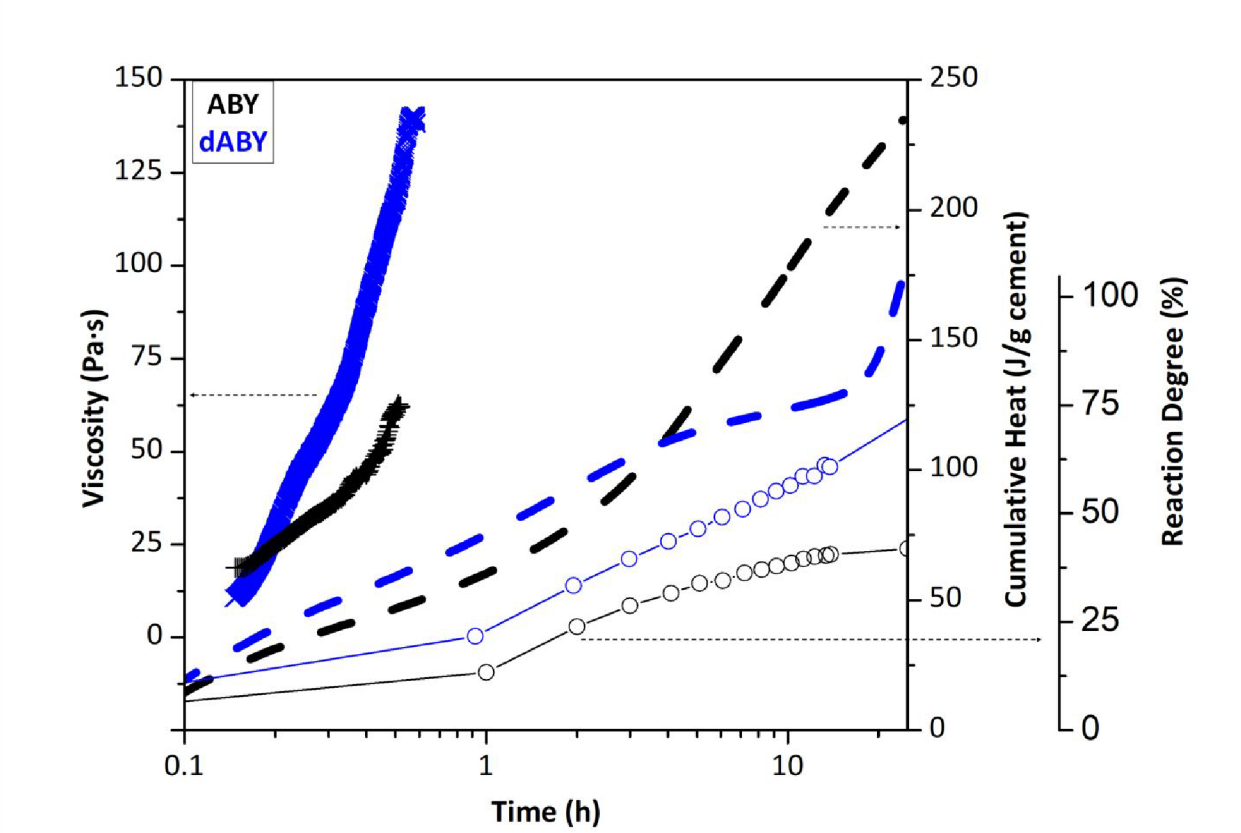

Figure 3. Viscosity as a function of time at the shear rate of 5 s^{-1} (left axis, crosses) reprinted in part) with permission from cement and concrete research 127 (2020) 105911. Copyright 2019 Elsevier Ltd., cumulative heat (right axis, dashed lines) and alite degree of reaction (right axis, circles) of ABY (black data) and dABY (blue data) pastes hydrated at w/c 0.5.

Role of boron on early hydration.

Borax was added to the raw meal to stabilize α'_H-form of C_2S[37,48]. The presence of boron on a cement paste initially retards the hydration[13] and this eventually causes an enhancement in mechanical properties when compared to those without the addition of boron[10]. Figure 4 shows the calorimetric curves of both cements hydrated at w/c of 0.5 for 7 days. On the one hand, the heat flow of ABY exhibits two broad signals centered at ~4.5 and ~10 hours of hydration mainly due to the dissolution of ye'elimite and hydration of alite, respectively. The total heat flow increases smoothly from the beginning due to the continuous ongoing hydration and precipitation reactions. On the other hand, dABY hydration is similar to that of ABY and at ~4 hours the heat evolved for both cements are coincident ~110 J/g, Figure 4. However, from 4 hours up to ~10 hours of hydration the heat released by dABY has increased up to ~125 J/g, which means 30% less than the increase of ABY (~175 J/g), Figure 4. This means that the addition of boron (modifying the dissolution rates and consequently the phase assemblage) has enlarged the open time of this cement, delaying the acceleration period up to ~15 hours. The signal centered at 24 hours is mainly due to the precipitation of amorphous aluminum hydroxide that has been delayed in this paste, Figure 5. At seven days of hydration the heat released of both cements are very similar.

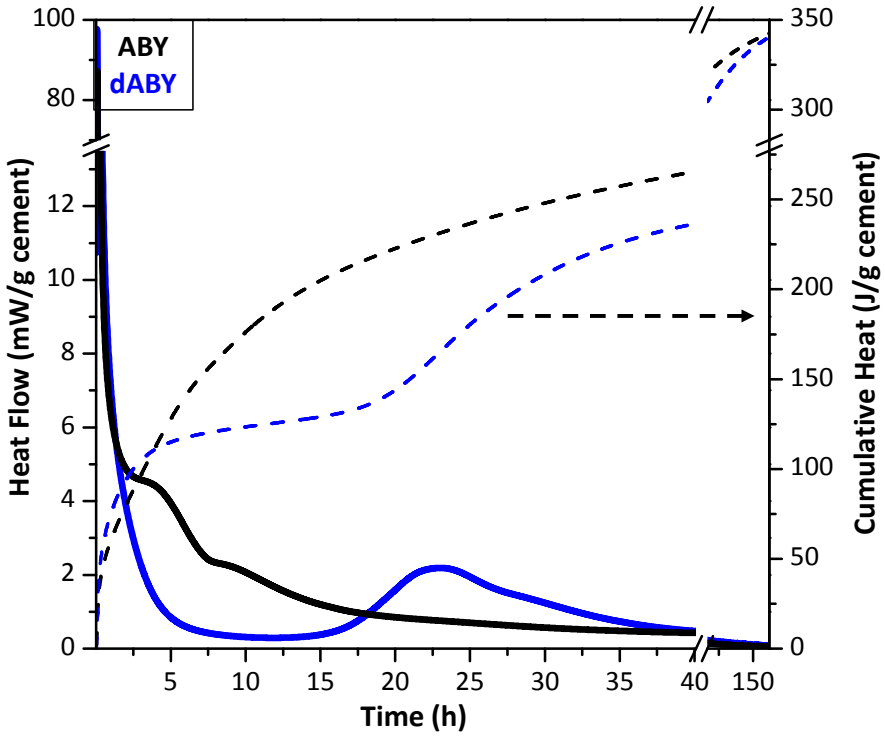

Figure 4. Calorimetric curves of ABY (black data) and dABY (blue data) hydrated at w/c of 0.5 up to 7 days.

3.3 Reactivity of aluminate and silicate phases.

Silicates (alite and different forms of belite) hydrate to give calcium silicate hydrates, mainly C-S-H gel[49] or stratlingite.[50] The latter is formed in systems with sources of aluminium and silicon like BYF cements.[10] However, in these ABY and dABY cements stratlingite was not formed at any hydration time, in agreement with other related systems[51] in which this phase is only formed in mixtures of PC with more than 50 wt% of calcium sulfoaluminate. Figure 5 gives normalized ^{27}Al MAS-NMR spectra for both anhydrous cements and hydrated pastes at 4, 15 and 24 hours jointly with 28 and 90 days. Aluminium in ye'elimite is evidenced as a broad peak in the anhydrous spectra with its maximum at 70 ppm in the anhydrous spectra. The absence of the Al(IV) peaks at ~61.9 and 68.5 ppm[52] in all the spectra confirms that stratlingite was not formed in these

experimental conditions, confirming XRPD results, Tables S1 and S2. The octahedrally coordinated Al present in ettringite, AH_3-gel and AFmare observed in the region from 0 to 20 ppm. Ettringite is deduced by its peak centred at 13.4 ppm, which corresponds to two non-resolved distinct Al sites in ettringite.[53] Moreover, the Al(VI) in AFm and AH_3 appears as broader signals centred in the range from 9 to 11 ppm due to their poor crystallinity. A clear difference is observed in the early hydration ^{27}Al spectra for ABY and dABY. The resonance of Al(VI) corresponding to AH_3-gel, close to 10 ppm, coming from the reaction of the aluminates (ye'elimite and mayenite) with anhydrite, is noticeable after 4 hours for ABY meanwhile it is not observed even at 24 hours for dABY, see right panel of Figure 5. In these experimental conditions, and due to the role of boron[13], the precipitation of aluminium hydroxide-gel has been delayed. No significant differences are observed when comparing ^{27}Al MAS-NMR spectra of ABY and dABY pastes after 28 and 90 days.

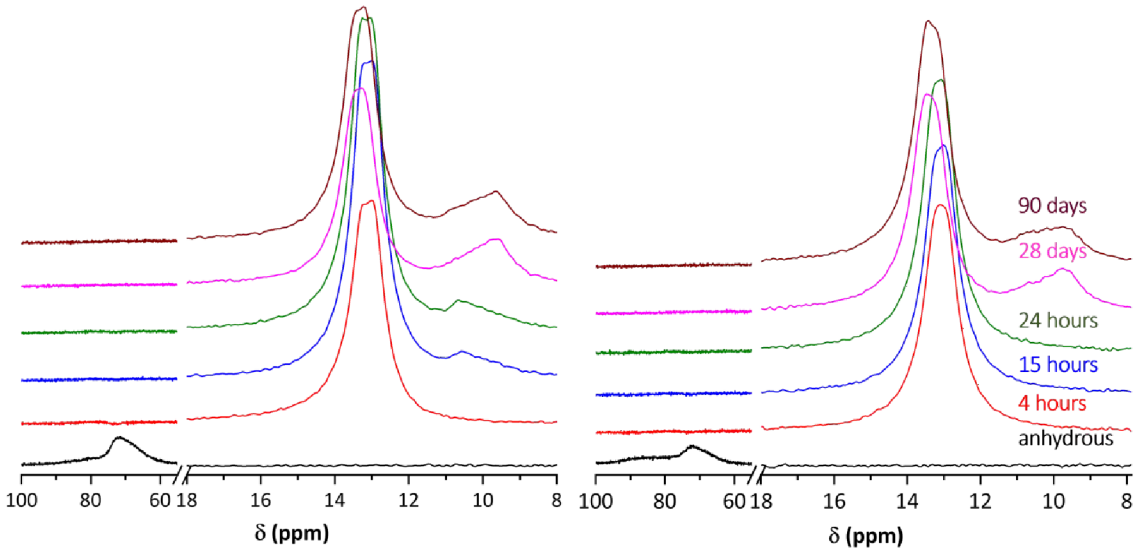

Figure 5. Normalized ^{27}Al MAS-NMR spectra for ABY (left) and dABY (right), anhydrous and after 4, 15 and 24 hours and 28 and 90 days of hydration.

ABY cement contains monoclinic M_3 C_3S and β-C_2S, while dABY also contains α'$_H$-C_2S. The hydration of C_3S gives C-S-H gel with Ca/Si~1.8.[54] However, the local structure and stoichiometric of C-S-H gel formed from belite is still under investigation. Table 2 gives the degree of hydration of silicate phases in both cements at later ages of hydration, derived from data given in Figure 2 and Tables S1 and S2. These results are in agreement with those obtained in the same systems but with the addition of superplasticizers[35] and indicate that alite in ABY cement reacted at all hydrated ages at a slightly higher pace than in dABY. Conversely and chiefly belite (both polymorphs) are more reactive in the boron-activated cement than in the neat one. This activation of the belite forms in dABY may be due the incorporation of boron in their frameworks that causes structural distortions, as observed previously with other dopants[17]. This observation is in disagreement with our previous results observed in a related system, BYF cements, in which β-belite degree of reaction was ~50% after 28 days meanwhile that of α'$_H$-form in boron-doped BYF was smaller, ~25%.[10] However, in spite of the lower reported reactivity of α'$_H$-form in doped BYF, the mechanical strengths were always higher[10] than those of non-doped BYF, mainly due to the formation of less stratlingite and consequently more C-S-H gel. In ABY and dABY cements, the hydration of alite and the different polymorphs of belite have yielded the formation of C-S-H gel, since stratlingite was not formed.

Table 2. Degree of hydration of silicate phases for the studied cements at 28 and 90 days derived from the RQPA results given in Figure 2 and Tables S1 and S2.

	ABY		dABY		
	M_3 C_3S	β-C_2S	M_3 C_3S	β-C_2S	α'$_H$-C_2S
7 d	85	15	83	19	49

28 d	95	42	83	**80**	**88**
90 d	94	59	81	85	86

*The estimated errors in the degree of reactions, based on the Rietveld quantitative analyses, are close to 4%.

Figure 6 displays ^{29}Si MAS-NMR spectra for ABY and dABY pastes with the corresponding deconvolutions. It has to be remarked that these spectra have been normalized for the sake of better visualisation. Figure S6 shows the raw spectra without any normalization for completeness. The first significant result is that the ^{29}Si MAS-NMR signal for anhydrous dABY is much broader than that for ABY indicating much large local disorder, which is due to the doping with boron and justifies the higher degree of hydration of belite forms. The second relevant result obtained from ^{29}Si MAS-NMR data is that amount of silicon-bearing hydrated phases after 28 days is much lower in ABY than in dABY pastes. From these data, mean chain lengths[55] (MCL) were calculated, being 6.1 and 6.0 at 28 days for ABY and dABY pastes, respectively. While, 5.0 and 3.9 were obtained at 90 days for ABY and dABY, respectively. These values are in agreement with previous publications for similar systems.[56,57] Moreover, these MCL values and the slight decrease of them with hydration time suggest that the C-S-H formed is calcium rich and should contain a Ca/Si ratio over 1.5,[58] but no significant differences are observed between both systems. The most conspicuous result obtained by ^{29}Si MAS-NMR is that dABY pastes have developed higher amount of C-S-H gel which implies a higher hydration degree of β- and α'_H belite, Table 2 and Figure 6. Moreover, a quantitative study has been performed by comparing the silicate rich phases obtained from RQPA and those ones obtained from ^{29}Si MAS-NMR data, Table 3. Table S3, given as Supporting Information, contains the quantitative analysis of the silicon rich phases of the

anhydrous materials obtained from XRD and ^{29}Si MAS-NMR. These values compared quite well ensuring the accuracy of the used methodologies.

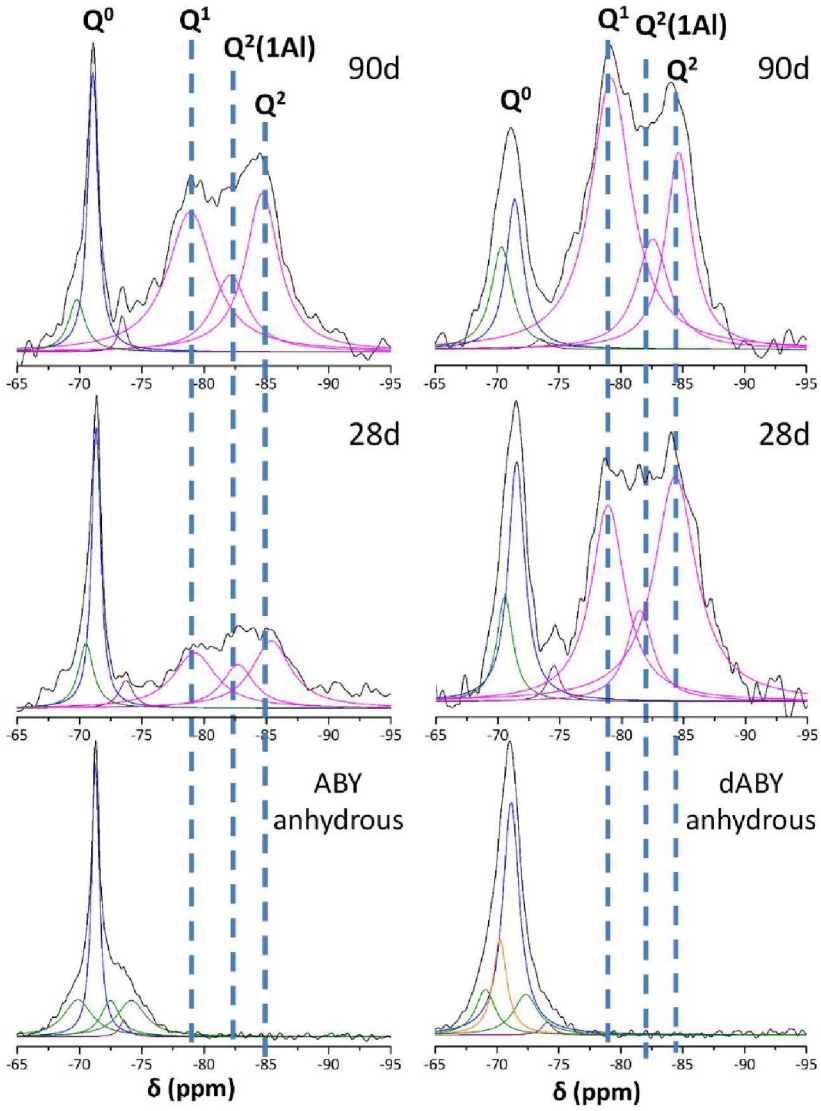

Figure 6. ^{29}Si MAS-NMR spectra of ABY (left panels) and dABY (right panels) with the deconvoluted signals included. Blue Q^0 for β-C_2S, orange Q^0 for α'$_H$-C_2S, green Q^0 for C_3S, purple Q^0 for F-ellestadite and pink Q^n for hydrated C-S-H.

Table 3. Quantitative phase analysis of the silicon rich fraction of ABY and dABY pastes at 28 and 90 days of hydration determined by XRPD and ^{29}Si MAS-NMR.

	28 d ABY		28 d dABY		90 d ABY		90 d dABY	
	XRD wt%	NMR wt%	XRD wt%	NMR wt%	XRD wt%	NMR wt%	XRD wt%	NMR wt%
C_3S	2	9	3	7	3	5	4	9
β-C_2S	24	24	9	15	16	15	7	10
α'_H-C_2S	-	-	2	-	-	-	2	-
F-elles	4	4	2	2	5	2	2	1
katoite	2	-	2	-	3	-	3	-
C-S-H_{C3S}	44*		16*		42*		16*	
C-S-$H_{\beta C2S}$	23*	63	48*	76	31*	80	51*	81
C-S-$H_{\alpha'HC2S}$	-		17*		-		17*	

*$(CaO)_{1.8}SiO_2(H_2O)_4$ stoichiometry has been used to derive the amount of gel formed from the hydration of alite, β-C_2S and α'_H-C_2S in each case.

The ACn value obtained from RQPA jointly with the internal standard method, Figure 2, is the total amount of amorphous, disordered or nanocrystalline fraction of the pastes. Consequently, in order to estimate the amount of isolated amorphous C-S-H gel, the stoichiometry $(CaO)_{1.8}SiO_2(H_2O)_4$ was assumed[54] for alite, β-C_2S and α'_H-C_2S hydration products, consequently the amount of amorphous C-S-H gel arising from each individual silicate phase is given in Table 3. The derived values under these assumptions are quite satisfactory, Table 3, when compared with those obtained from ^{29}Si MAS-NMR, in which no approximations are needed, as the total area of the signals in Figure 6 are measured.

Finally, it is informative to compare these results with the mechanical strengths developed by these cements. The degree of reaction of these pastes without any superplasticizer is similar to that

determined for the same cements with the addition of superplasticizers[35], confirming that the addition of superplasticizers affects the early kinetic of hydration but not the long term phase assemblage. The compressive mechanical strengths developed by ABY mortars (w/c of 0.5 and 0.4 wt% of superplasticizer[35]) were 29.9(5), 43(2), 45(1) and 57(3) MPa at 1, 7, 28 and 56 days respectively; while those for dABY (w/c of 0.5 and 0.4 wt% of superplasticizer[35]) were 17(2), 40.7(2), 75(2) and 82(2) MPa for the same ages. After one day of hydration, ABY paste developed higher mechanical strengths than dABY. This is related to the larger degree of reaction of ABY pastes up to 24 hours, as shown in the higher heat of hydration (234 and 174 J/g, for ABY and dABY, respectively) Figure 4. Moreover, the precipitation of AH_3-gel at early hours of hydration, Figure 5, also supports the higher mechanical strengths. . However, at later ages, dABY mortars show a greater increase in the development of compressive mechanical strengths, mainly due to the higher hydration degree of β-C_2S and α'$_H$-C_2S which yielded larger amounts of C-S-H gel. It must be highlighted that the jump in mechanical strength of dABY clearly correlated with the leap in reaction degree of belites.

Conclusions

The production of alite-belite-ye'elimite (ABY) cements released up to 17% less carbon dioxide into atmosphere than PC production. The early hydration of these two containing cements is dependent on the fineness of the materials and on the amount of calcium (sulfo)aluminates. Specifically, ABY paste presented higher viscosity during the first 10 minutes of hydration likely due to slightly smaller particle sizes (higher Blaine parameter) and slightly higher amount of total ye'elimite. After that time, the higher amount of mayenite in dABY paste provokes the increase in reactivity and consequently in viscosity and heat released up to 3 hours. Moreover, alite hydration

is strongly affected by the amount of ye'elimite, i.e. the higher amount of ye'elimite in ABY paste is the responsible of the slower reactivity of alite in this paste.

This study shows that the addition of borax in the dABY has played two roles; i) delaying the precipitation of aluminium hydroxide gel up to more than 24 hours and ii) accelerating the reactivity of β-C_2S and α'$_H$-C_2S in dABY at later ages (activation effect). The delayed precipitation of AH_3-gel, due to the presence of boron in dABY, justifies the lower mechanical strengths of this cement after 1 day of hydration. Belite reaction degrees for dABY are higher than that of β-C_2S in ABY and consequently, the mechanical properties have been enhanced from 28 to 56 days of hydration for dABY.

In both systems, the hydration product of alite and all polymorphs of belite is C-S-H gel as no stratlingite was found at any hydration time (confirmed by XRD and ^{27}Al MAS-NMR). The nature of this C-S-H gel seems to be similar in both systems, although dABY paste has shown higher degree of reaction of both belite polymorphs (β and α'$_H$) and consequently higher amount of C-S-H gel has been formed.

Author Contributions

This work is part of the PhD of J.D.Z.-G.; A.G.DlT. and I.S designed the research; O.V. performed the SXRPD data collection; S.G.S. performed the calorimetric measurements; laboratory work were carried out by J.D.Z.-G.; A.G.DlT.; I.S. and M.A.G.A. J.D.Z.-G. and A.G.DlT. wrote the manuscript, which was revised and edited by all the authors.

Funding Sources

This research has been supported by Spanish MINECO and FEDER [BIA2017-82391-R research project and I3 (IEDI-2016-0079) program].

Supporting information

Supplementary Information includes tables with full phase assemblage (obtained from Rietveld Refinement with internal standard method and DTA-TG) of ABY and dABY (Tables S1 and S2), the quantitative phase analysis of silicon bearing phases of anhydrous ABY and dABY cements obtained by XRD & Rietveld method and ^{29}Si MAS-NMR (Table S3). Six figures are also included: PSD of ABY and dABY (Figure S1), SXRPD and LXRPD raw patterns of hydrated pastes (Figures S2 and S3), Rietveld plots of pastes hydrated at 1 and 14 hours (Figures S4 and S5) and ^{29}Si MAS-NMR and ^{27}Al MAS-NMR raw spectra (Figure S6).

All the raw patterns and spectra analysed in this article are openly deposited in Zenodo at https://doi.org/10.5281/zenodo.3367442.

References

(1) Amato, I. Green Cement: Concrete Solutions. *Nature* **2013**, *494* (7437), 300–301.

(2) UN Environment; Scrivener, K. L.; John, V. M.; Gartner, E. Eco-Efficient Cements: Potential, Economically Viable Solutions for a Low-CO2, Cement-Based Materials Industry. *Cem. Concr. Res.* **2018**, *114*, 2–26.

(3) Barcelo, L.; Kline, J.; Walenta, G.; Gartner, E. Cement and Carbon Emissions. *Mater. Struct.* **2014**, *47* (6), 1055–1065.

(4) Gartner, E.; Hirao, H. A Review of Alternative Approaches to the Reduction of CO2 Emissions Associated with the Manufacture of the Binder in Concrete. *Cem. Concr. Res.* **2015**, *78*, 126–142.

(5) Juenger, M. C. G.; Snellings, R.; Bernal, S. A. Supplementary Cementitious Materials: New

Sources, Characterization, and Performance Insights. *Cem. Concr. Res.* **2019**, *122*, 257–273.

(6) Belz, G.; Beretka, J.; Marroccoli, M.; Santoro, L.; Sherman, N.; Valenti, G. L. Use of Fly Ash, Blast Furnace Slag, and Chemical Gypsum for the Synthesis of Calcium Sulfoaluminate-Based Cements. *Spec. Publ.* **1995**, *153*, 513–530.

(7) Aranda, M. A. G.; De la Torre, A. G. Sulfoaluminate Cement in Eco-Efficient Concrete; Pacheco-Torgal, F. Ed.; Jalali, S. Ed. Labrincha, J. Ed. *Woodhead Publ. Cambridge* **2013**, 488–522.

(8) Morin, V.; Termkhajornkit, P.; Huet, B.; Pham, G. Impact of Quantity of Anhydrite, Water to Binder Ratio, Fineness on Kinetics and Phase Assemblage of Belite-Ye'elimite-Ferrite Cement. *Cem. Concr. Res.* **2017**, *99*, 8–17.

(9) Li, C.; Wu, M.; Yao, W. Eco-Efficient Cementitious System Consisting of Belite-Ye'elimite-Ferrite Cement, Limestone Filler, and Silica Fume. *ACS Sustain. Chem. Eng.* **2019**, *7*, 7941–7950.

(10) Álvarez-Pinazo, G.; Santacruz, I.; León-Reina, L.; Aranda, M. A. G.; De La Torre, A. G. Hydration Reactions and Mechanical Strength Developments of Iron-Rich Sulfobelite Eco-Cements. *Ind. Eng. Chem. Res.* **2013**, *52* (47), 16606–16614.

(11) Gartner, E. M. What Are BYF Cements, and How Do They Differ from CSA Cements? In *The Future of Cement, 200 years after Louis Vicat, UNESCO.*; Paris, 2017; pp 1–9.

(12) Ben Haha, M.; Winnefeld, F.; Pisch, A. Advances in Understanding Ye'elimite-Rich Cements. *Cem. Concr. Res.* **2019**, *123*, 105778.

(13) Bullerjahn, F.; Zajac, M.; Skocek, J.; Ben Haha, M. The Role of Boron during the Early Hydration of Belite Ye'elimite Ferrite Cements. *Constr. Build. Mater.* **2019**, *215*, 252–263.

(14) Gastaldi, D.; Bertola, F.; Canonico, F.; Buzzi, L.; Mutke, S.; Irico, S.; Paul, G.; Marchese, L.; Boccaleri, E. A Chemical/Mineralogical Investigation of the Behavior of Sulfoaluminate Binders Submitted to Accelerated Carbonation. *Cem. Concr. Res.* **2018**, *109*, 30–41.

(15) Walenta, G.; Comparet, C.; Morin, V.; Gartner, E. Hydraulic Binder Based on Sulfoaluminate Clinker and Minerals Additions. World Patent Application WO. 2010/070215 A1., 2010.

(16) Bullerjahn, F.; Schmitt, D.; Ben Haha, M. Effect of Raw Mix Design and of Clinkering Process on the Formation and Mineralogical Composition of (Ternesite) Belite Calcium Sulphoaluminate Ferrite Clinker. *Cem. Concr. Res.* **2014**, *59*, 87–95.

(17) Morsli, K.; De La Torre, A. G.; Stöber, S.; Cuberos, A. J. M.; Zahir, M.; Aranda, M. A. G. Quantitative Phase Analysis of Laboratory-Active Belite Clinkers by Synchrotron Powder Diffraction. *J. Am. Ceram. Soc.* **2007**, *90* (10), 3205–3212.

(18) Kim, Y. M.; Hong, S. H. Influence of Minor Ions on the Stability and Hydration Rates of β-Dicalcium Silicate. *J. Am. Ceram. Soc.* **2004**, *87* (5), 900–905.

(19) Shen, Y.; Qian, J.; Huang, Y.; Yang, D. Synthesis of Belite Sulfoaluminate-Ternesite Cements with Phosphogypsum. *Cem. Concr. Compos.* **2015**, *63*, 67–75.

(20) Park, C.-K. Phase Transformation and Hydration of Dicalcium Silicate Containing Stabilizers. *J. Ceram. Soc. Japan* **2001**, *109* (1269), 380–385.

(21) Chitvoranund, N.; Lothenbach, B.; Winnefeld, F.; Hargis, C. W. Synthesis and Hydration

of Alite-Calcium Sulfoaluminate Cement. *Adv. Cem. Res.* **2016**, *29* (3), 101–111.

(22) Ma, S.; Snellings, R.; Li, X.; Shen, X.; Scrivener, K. L. Alite-Ye'elimite Cement: Synthesis and Mineralogical Analysis. *Cem. Concr. Res.* **2013**, *45*, 15–20.

(23) Lili, R.; Xiaocun, L.; Tao, Q.; Jian, L.; Deli, Z.; Yanjun, L. Influence of MnO2 on the Burnability and Mineral Formation of Alite-Sulphoaluminate Cement Clinker. *Silic. Ind.* **2009**, *74* (7–8), 183–188.

(24) Londono-Zuluaga, D.; Tobon, J. I.; Aranda, M. A. G.; Santacruz, I.; De La Torre, A. G. Clinkering and Hydration of Belite-Alite-Ye´elimite Cement. *Cem. Concr. Compos.* **2017**, *80*, 333–341.

(25) De La Torre, Á. G.; Cuberos, A. J. M.; Álvarez-Pinazo, G.; Cuesta, A.; Aranda, M. A. G. In Situ Powder Diffraction Study of Belite Sulfoaluminate Clinkering. *J. Synchrotron Radiat.* **2011**, *18* (3), 506–514.

(26) Altun, I. A. Effect of CaF2 and MgO on Sintering of Cement Clinker. *Cem. Concr. Res.* **1999**, *29* (11), 1847–1850.

(27) Li, J. H.; Ma, H. W.; Zhao, H. W. Preparation of Sulphoaluminate-Alite Composite Mineralogical Phase Cement Clinker from High Alumina Fly Ash. *Key Eng. Mater.* **2007**, *334–335*, 421–424.

(28) Ludwig, H.-M.; Zhang, W. Research Review of Cement Clinker Chemistry. *Cem. Concr. Res.* **2015**, *78*, 24–37.

(29) Li, X.; Shen, X.; Xu, J.; Li, X.; Ma, S. Hydration Properties of the Alite – Ye'elimite Cement Clinker Synthesized by Reformation. *Constr. Build. Mater.* **2015**, *99* (November 2015),

254–259.

(30) Zhang, H.; Odler, I. Investigations on High SO3 Portland Clinkers and Cements II. Properties of Cements. *Cem. Concr. Res.* **1996**, *26* (9), 1315–1324.

(31) Pérez-Bravo, R.; Losilla, E. R.; Álvarez-Pinazo, G.; Bruque, S.; Compana, J. M.; De La Torre, A. G.; Santacruz, I. Alite Sulfoaluminate Clinker: Rietveld Mineralogical and SEM-EDX Analysis. *Adv. Cem. Res.* **2014**, *26* (1), 10–20.

(32) Ma, B.; Li, X.; Shen, X.; Mao, Y.; Huang, H. Enhancing the Addition of Fly Ash from Thermal Power Plants in Activated High Belite Sulfoaluminate Cement. *Constr. Build. Mater.* **2014**, *52*, 261–266.

(33) Staněk, T.; Sulovský, P. The Influence of the Alite Polymorphism on the Strength of the Portland Cement. *Cem. Concr. Res.* **2002**, *32* (7), 1169–1175.

(34) García-Maté, M.; Santacruz, I.; De La Torre, Á. G.; León-Reina, L.; Aranda, M. A. G. Rheological and Hydration Characterization of Calcium Sulfoaluminate Cement Pastes. *Cem. Concr. Compos.* **2012**, *34* (5), 684–691.

(35) Zea-Garcia, J. D.; de la Torre, A. G.; Aranda, M. A. G.; Santacruz, I. Processing Optimisation and Characterisation of Standard and Doped Alite-Belite-Ye'elimite Ecocement Pastes and Mortars. *Cem. Concr. Res.* **2020**, *127*, 105911.

(36) Hu, Y.; Li, W.; Ma, S.; Shen, X. Influence of Borax and Citric Acid on the Hydration of Calcium Sulfoaluminate Cement. *Chem. Pap.* **2017**, *71* (10), 1909–1919.

(37) Zea-Garcia, J. D.; Santacruz, I.; Aranda, M. A. G.; De la Torre, A. G. Alite-Belite-Ye'elimite Cements: Effect of Dopants on the Clinker Phase Composition and Properties.

Cem. Concr. Res. **2019**, *115*, 192–202.

(38) De la Torre, A. G.; Santacruz, I.; Cuesta, A.; León-Reina, L.; Aranda, M. A. G. Diffraction and Crystallography Applied to Anhydrous Cements. In *Cementitious Materials. Composition, Properties, Application*; Pöllmann, H., Ed.; De Gruyter Publising: Berlin, Germany, 2017; pp 3–29.

(39) Fauth, F.; Peral, I.; Popescu, C.; Knapp, M. The New Material Science Powder Diffraction Beamline at ALBA Synchrotron. *Powder Diffr.* **2013**, *28* (S2), S360–S370.

(40) Von Dreele, R. B.; Larson, A. C. General Structure Analysis System (GSAS). *Los Alamos Natl. Lab. Rep. LAUR* **2004**, *748*, 86–748.

(41) Thompson, P.; Cox, D. E.; Hastings, J. B. Rietveld Refinement of Debye-Scherrer Synchrotron X-Ray Data from A1203. *J. Appl. Crystallogr.* **1987**, *20* (2), 79–83.

(42) Finger, L. W.; Cox, D. E.; Jephcoat, A. P. Correction for Powder Diffraction Peak Asymmetry Due to Axial Divergence. *J. Appl. Crystallogr.* **1994**, *27* (pt 6), 892–900.

(43) Jansen, D.; Goetz-Neunhoeffer, F.; Stabler, C.; Neubauer, J. A Remastered External Standard Method Applied to the Quantification of Early OPC Hydration. *Cem. Concr. Res.* **2011**, *41* (6), 602–608.

(44) Massiot, D.; Fayon, F.; Capron, M.; King, I.; Le Calvé, S.; Alonso, B.; Durand, J.-O.; Bujoli, B.; Gan, Z.; Hoatson, G. Modelling One- and Two-Dimensional Solid-State NMR Spectra. *Magn. Reson. Chem.* **2002**, *40* (1), 70–76.

(45) Bullerjahn, F.; Zajac, M.; Ben Haha, M.; Scrivener, K. L. Factors Influencing the Hydration Kinetics of Ye'elimite; Effect of Mayenite. *Cem. Concr. Res.* **2019**, *116*, 113–119.

(46) Pelletier-Chaignat, L.; Winnefeld, F.; Lothenbach, B.; Saout, G. Le; Müller, C. J.; Famy, C. Influence of the Calcium Sulphate Source on the Hydration Mechanism of Portland Cement-Calcium Sulphoaluminate Clinker-Calcium Sulphate Binders. *Cem. Concr. Compos.* **2011**, *33* (5), 551–561.

(47) Hanein, T.; Duvallet, T. Y.; Jewell, R. B.; Oberlink, A. E.; Robl, T. L.; Zhou, Y.; Glasser, F. P.; Bannerman, M. N. **Alite Calcium Sulfoaluminate Cement: Chemistry and Thermodynamics**. *Adv. Cem. Res.* **2019**, *31* (3), 94–105.

(48) Cuesta, A.; Losilla, E. R.; Aranda, M. A. G.; Sanz, J.; De La Torre, A. G. Reactive Belite Stabilization Mechanisms by Boron-Bearing Dopants. *Cem. Concr. Res.* **2012**, *42* (4), 598–606.

(49) Zhang, X.; Chang, W.; Zhang, T.; Ong, C. K. Nanostructure of Calcium Silicate Hydrate Gels in Cement Paste. *J. Am. Ceram. Soc.* **2004**, *83* (10), 2600–2604.

(50) Kwan, S.; LaRosa, J.; Grutzeck, M. W. 29Si and 27Al MASNMR Study of Stratlingite. *J. Am. Ceram. Soc.* **1995**, *78* (7), 1921–1926.

(51) Trauchessec, R.; Mechling, J. M.; Lecomte, A.; Roux, A.; Le Rolland, B. Hydration of Ordinary Portland Cement and Calcium Sulfoaluminate Cement Blends. *Cem. Concr. Compos.* **2015**, *56*, 106–114.

(52) Rinaldi, R.; Sacerdoti, M.; Passaglia, E. Strätlingite: Crystal Structure, Chemistry, and a Reexamination of Its Polytpye Vertumnite. *Eur. J. Mineral.* **1990**, *2* (6), 841–850.

(53) Skibsted, J.; Pedersen, M. T.; Holzinger, J. Resolution of the Two Aluminum Sites in Ettringite by ^{27} Al MAS and MQMAS NMR at Very High Magnetic Field (22.3 T). *J. Phys.*

Chem. C **2017**, *121* (7), 4011–4017.

(54) Cuesta, A.; Zea-Garcia, J. D.; Londono-Zuluaga, D.; De la Torre, A. G.; Santacruz, I.; Vallcorba, O.; Dapiaggi, M.; Sanfélix, S. G.; Aranda, M. A. G. Multiscale Understanding of Tricalcium Silicate Hydration Reactions. *Sci. Rep.* **2018**, *8* (1), 8544.

(55) Richardson, I. . The Nature of C-S-H in Hardened Cements. *Cem. Concr. Res.* **1999**, *29* (8), 1131–1147.

(56) Gastaldi, D.; Paul, G.; Marchese, L.; Irico, S.; Boccaleri, E.; Mutke, S.; Buzzi, L.; Canonico, F. Hydration Products in Sulfoaluminate Cements: Evaluation of Amorphous Phases by XRD/Solid-State NMR. *Cem. Concr. Res.* **2016**, *90*, 162–173.

(57) Le Saoût, G.; Lothenbach, B.; Hori, A.; Higuchi, T.; Winnefeld, F. Hydration of Portland Cement with Additions of Calcium Sulfoaluminates. *Cem. Concr. Res.* **2013**, *43*, 81–94.

(58) Kunther, W.; Ferreiro, S.; Skibsted, J. Influence of the Ca/Si Ratio on the Compressive Strength of Cementitious Calcium–Silicate–Hydrate Binders. *J. Mater. Chem. A* **2017**, *5* (33), 17401–17412.

For Table of Contents Use Only

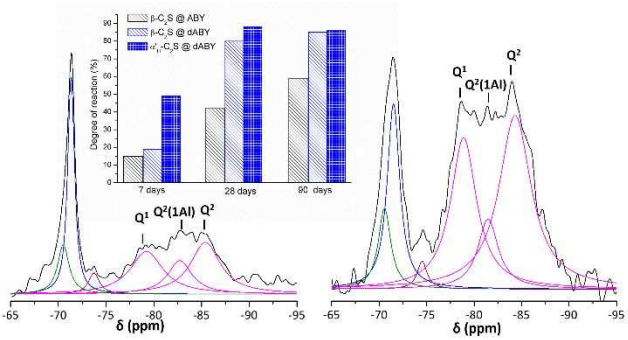

The main phases of cements emitting ~17% less CO_2 (dABY) in their clinkering process, present higher degree of reaction at all ages and developed higher amounts of C-S-H gel, contributing to higher mechanical strengths.

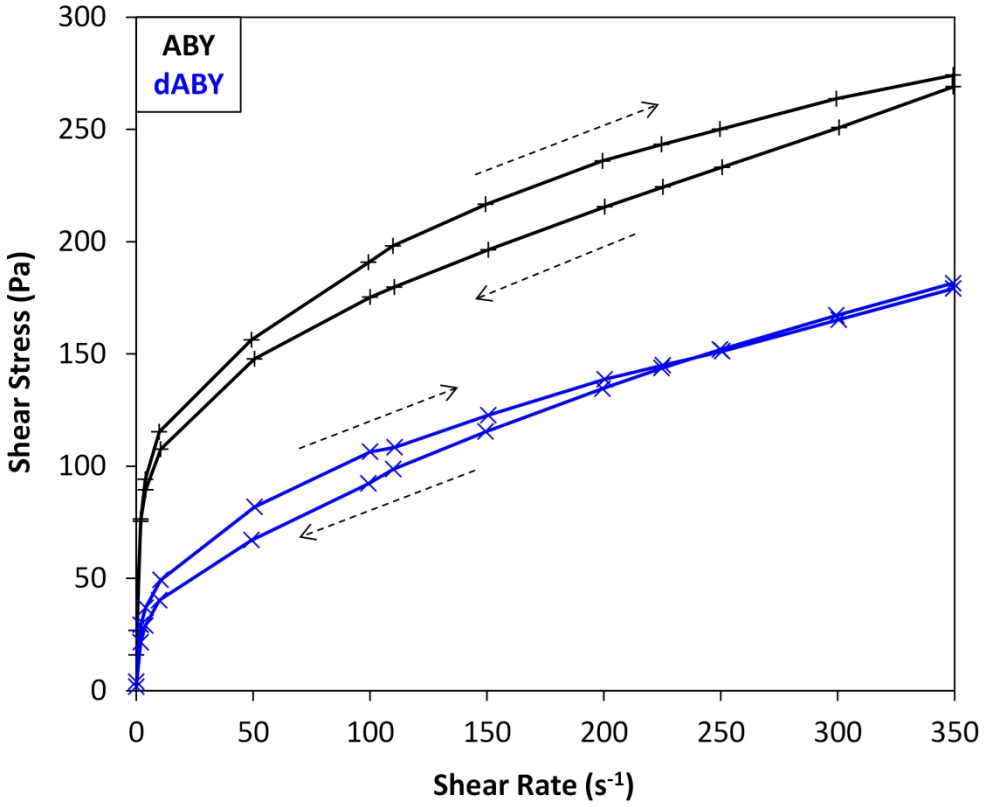

Figure 1. Flow curves for ABY and dABY pastes at w/c of 0.5. ABY in black; dABY in blue.

460x396mm (150 x 150 DPI)

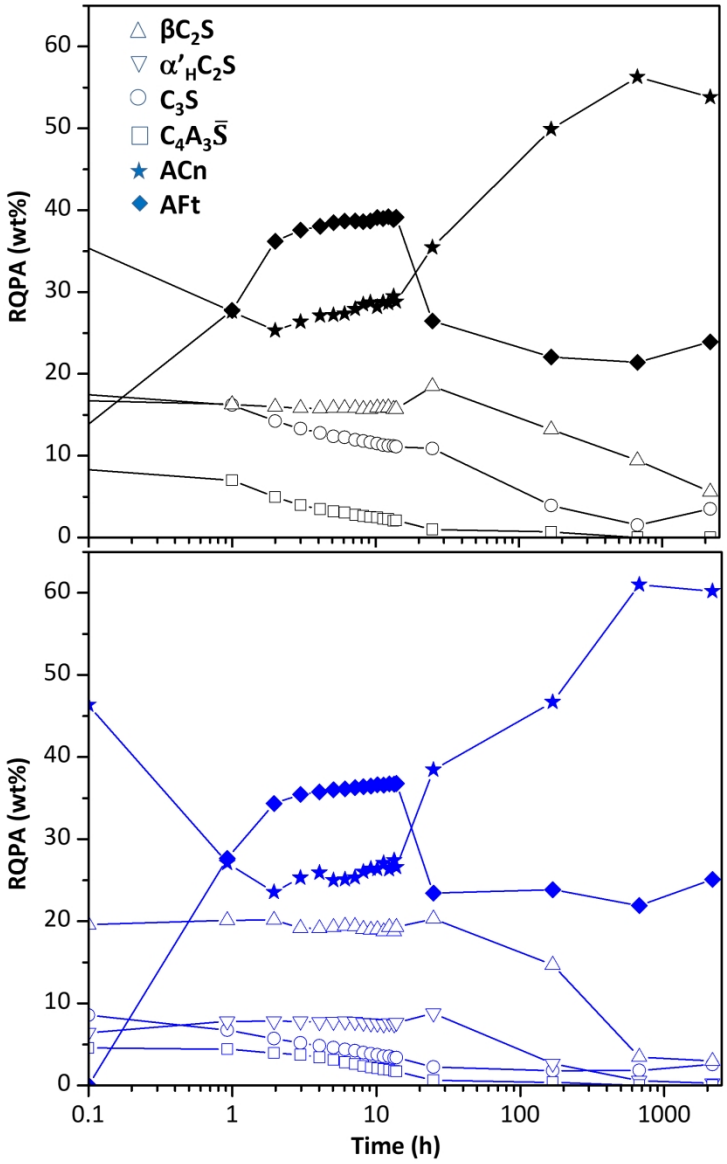

Figure 2. Phase assemblage as a function of time for ABY (up) and dABY (down), where only main phases are plotted.

345x531mm (150 x 150 DPI)

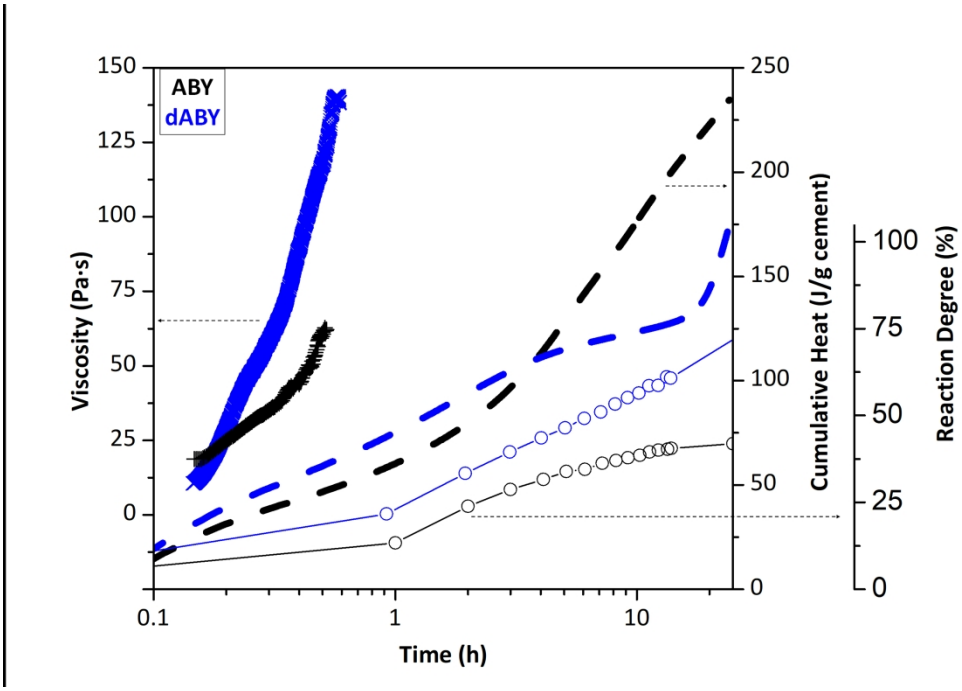

Figure 3. Viscosity as a function of time at the shear rate of 5 s-1 (left axis, crosses) reprinted in part) with permission from cement and concrete research 127 (2020) 105911. Copyright 2019 Elsevier Ltd., cumulative heat (right axis, dashed lines) and alite degree of reaction (right axis, circles) of ABY (black data) and dABY (blue data) pastes hydrated at w/c 0.5.

872x596mm (150 x 150 DPI)

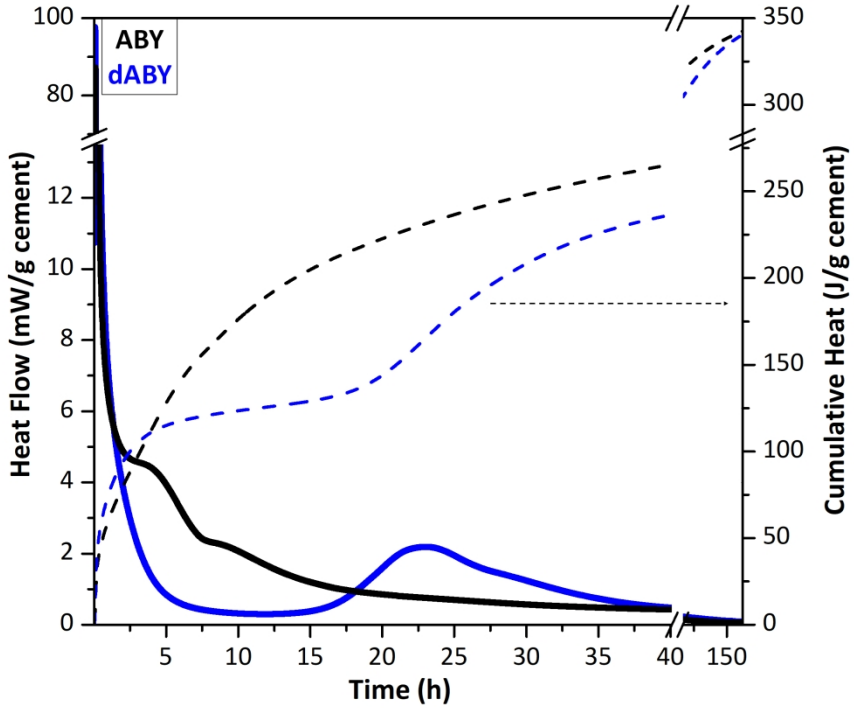

Figure 4. Calorimetric curves of ABY (black data) and dABY (blue data) hydrated at w/c of 0.5 up to 7 days.

752x576mm (97 x 97 DPI)

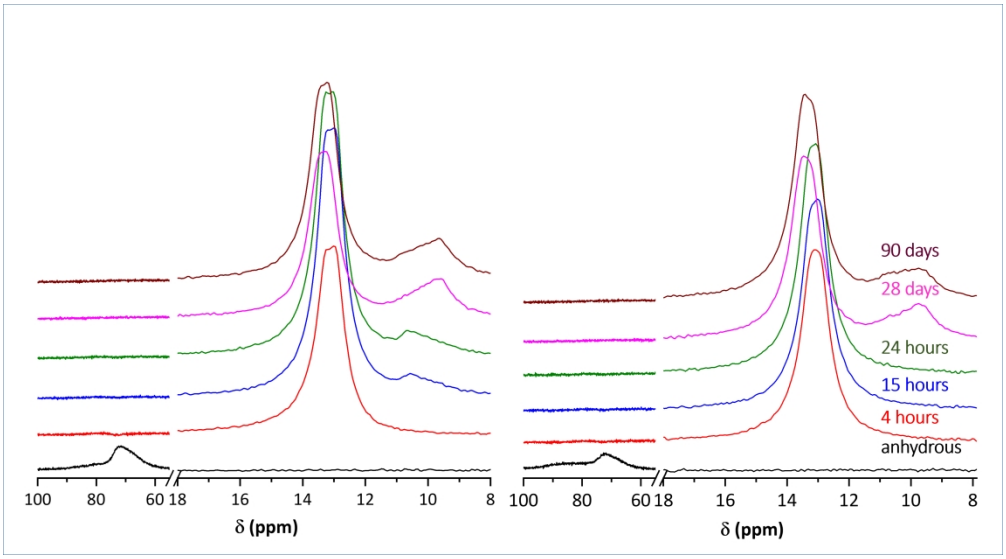

Figure 5. Normalized 27Al MAS-NMR spectra for ABY (left) and dABY (right), anhydrous and after 4, 15 and 24 hours and 28 and 90 days of hydration.

754x415mm (150 x 150 DPI)

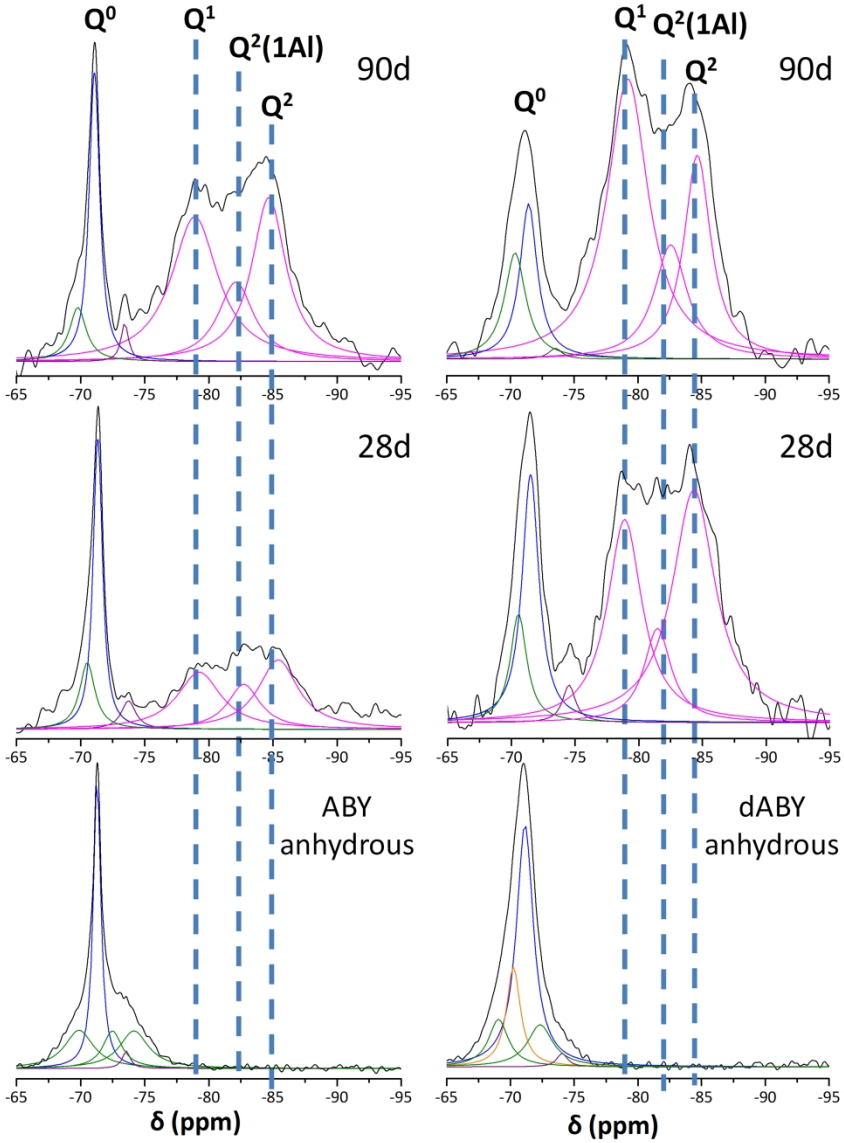

Figure 6. 29Si MAS-NMR spectra of ABY (left panels) and dABY (right panels) with the deconvoluted signals included. Blue Q0 for β-C2S, orange Q0 for α'H-C2S, green Q0 for C3S, purple Q0 for F-ellestadite and pink Qn for hydrated C-S-H.

796x1065mm (150 x 150 DPI)